JOURNAL OF NANO- AND ELECTRONIC PHYSICS
Vol. **9** No 4, 04005(6pp) (2017)

ЖУРНАЛ НАНО- ТА ЕЛЕКТРОННОЇ ФІЗИКИ
Том **9** № 4, 04005(6cc) (2017)

A Simple Approach on Synthesis of TiO_2 Nanoparticles and its Application in dye Sensitized Solar Cells

L.S. Chougala[1], M.S. Yatnatti[1], R.K. Linganagoudar[2], R.R. Kamble[3], J.S. Kadadevarmath[1,*]

[1] *Department of Physics, Karnatak University, Dharwad-580 003, Karnataka, India*
[2] *Department of Electronics, Karnatak University, Dharwad-580 003, Karnataka, India*
[3] *Department of Chemistry, Karnatak University, Dharwad-580003, Karnataka, India*

(Received 15 March 2017; published online 27 July 2017)

This paper presents a simple, low cost method of synthesizing TiO_2 nanoparticles by sol-gel method, where titanium isopropoxide is used as a starting material. Further, same TiO_2 is used to sensitize 2-cyano-3- (4-(7-(5-(4- (diphenylamino) phenyl)-4- octylthiophen-2-yl) benzo[c] [1, 2, 5] thiadiazol-4-yl)phenyl) acrylic acid (RK-1 dye) and Di-tetrabutylammonium cis-bis (isothiocyanato) bis (2,2'-bipyridyl-4,4'-dicarboxylato) ruthenium(II) (N-719 dye) for light harvesting applications. Anatase structure and average particle size of 7.3 nm were confirmed from XRD pattern. From SEM, it was noticed that particles were of varying size and shape and aggregation with clear porosity. FTIR spectra reveal Ti-O bond corresponding to 483 cm^{-1} and from UV-Vis absorption, energy band gap was found to be 3.2 eV. Photocurrent density (J) - photovoltage (V) characteristic of DSSC of different thicknesses of TiO_2 were obtained, it was observed that optimum solar energy to electricity conversion efficiency (η) for RK-1 dye and N- 719 dye 4.08 % and 5.12 % with TiO_2 thickness of 5.4 µm and 8.6 µm respectively under AM 1.5 irradiation (1000 W/m^2) conditions.

Keywords: TiO_2 nanoparticles, Dye sensitized solar cells (DSSCs), Short circuit current density (J_{sc}), Efficiency (η).

DOI: 10.21272/jnep.9(4).04005 PACS numbers: 78.67.Bf, 84.60.Jt

1. INTRODUCTION

Titanium dioxide (TiO_2) is one of the most attractive wide band gap semiconductors (transition-metal oxide), non-toxic, highly stable, photo-active and absorbs light in UV region [1]. TiO_2 exhibits corrosion resistance, good physical and chemical properties and considered promising material for solar cell applications and also used for fluorescence quencher, biological sensor and medical diagnosis etc [2]. TiO_2 nanoparticles are almost popular materials for preparing DSSC photo-anodes made with different shapes of TiO_2 nanostructures such as nanorods [3, 4], nanotubes [5, 6] and nanofibers [7], etc and demonstrated their own advantages. Most of the research focuses on modified properties of TiO_2 structures, morphology [8, 9], tuning of the phase [10] or external doping [11, 12] by different approaches. TiO_2 nanoparticles morphology, specific surface area, crystal phase and crystalline structure play an important role in solar cell performance [13].

As silicon based solar cells have some disadvantages, such as high fabrication cost and release of hazardous gasses during fabrication lead the researchers to think for alternative solar cells [14]. Dye-sensitized solar cell (DSSC) is one of the alternative solar cells which is a electrochemical photonic device convert solar energy directly into electrical energy and it can produce clean renewable energy (electricity). Dye sensitized solar cell (DSSC) is low cost device and environmentally friendly [15]. In DSSC applications reduction in the size of the TiO_2 nanostructured particles can i) enhance the surface area, ii) shorten electron diffusion length and iii) yield poor light scattering ability. Larger surface area may provide better attachment of a dye however, the density of grain boundaries and defect sites retard the electron transport [13, 16]. Larger nanoparticles have a longer electron diffusion length with higher light scattering ability but lower surface area. So, there is an optimal particle size for the best efficiency and that has been known as 15 ~ 20 nm in diameter [13]. Further, the photovoltaic performance may be studied as function of TiO_2 film thickness. It is noticed that overall power conversion efficiency (PCE) of a cell sensitized by pyronine G (PYR) dye has been increased as function thickness of TiO_2. This may be attributed to the more dye adsorption which leads to more photon absorption resulting higher photocurrent [17]. TiO_2 nanoparticles can be synthesized by a several methods such as sol-gel, hydrothermal, micro-emulsion, thermal decomposition of alkoxides, and etc [18]. Usually TiO_2 nanoparticles were synthesized by a sol-gel process followed by hydrothermal treatment [19, 20] for DSSC applications. The hydrothermal treatment leads to prominent particle growths, which significantly decreases the surface area of nanoparticles and dye attachment on nanoparticles. Hydrothermal treatment is hazardous and energy consuming, which should be avoided in large-scale production. The concern at this point is to avoid hazardous, enhancement of surface area and PCE of cell as a result of more dye adsorption.

Keeping these concerns in view, it is proposed to synthesize TiO_2 nanoparticles by sol-gel method without hydrothermal route which is considered as less expensive simple method. Same synthesized TiO_2 nanoparticles were characterized using X-ray diffraction (XRD), fourier transform infrared spectroscopy (FTIR), scanning electron microscope (SEM) with energy dispersive analysis of X-ray (EDAX), atomic force microscopy

* jagadishsk1956@gmail.com

(AFM) and UV-Vis NIR absorption spectrometer and subsequently used to prepare photo-anodes of DSSCs.

2. EXPERIMENTAL DETAILS

2.1 Materials Used

Titanium isopropoxide, Di-tetrabutyl ammoniumcis-bis (isothiocyanato) bis (2,2'-bipyridyl-4,4'-dicarboxylato) ruthenium(II) (N-719 dye) and 4-tert-Butylpyridine (TBP) were procured from Sigma Aldrich. Triton X-100, Iodine and Lithium Iodide were procured from HiMedia laboratory and Alfa Aesar respectively. 2-cyano-3-(4-(7-(5-(4- (diphenylamino)phenyl) -4-octylthiophen-2-yl)benzo[c][1,2,5] thiadiazol-4-yl)phenyl) acrylic acid (RK-1 dye), Di Methyl 3-Propyl ImidAzolium Iodide (DMPII), Fluorine doped tin oxide (FTO) glasses and Pilkington Nippon Sheet Glass (NSG) (thickness of 2.2 mm, (80 % visible light transmission and 7 Ω/sq sheet resistance) were procured from Solaranix. AR grade solvents such as ethanol and acetonitrile were used. Milli Q water (distilled water) was used.

2.2 Methods of Characterization of Synthesized TiO_2 Nanoparticles

XRD, FTIR, SEM with EDAX, AFM and absorption measurements were carried out using Bruker D8 Discover diffractometer (CuKα radiation ($\lambda = 1.5406$ Å)), IMPACT-410 Nicolet (USA), Nova Nano scanning electron microscope 600 with EDAX (FEI Co., Netherlands), Nanosurf Naio atomic force microscopy and UV-Vis NIR spectrophotometer (JASCO V-670, Japan) instruments respectively.

2.3 Photocurrent Density (J) - photovoltage (V) and Thickness of TiO_2 Film Measurements

Photocurrent density (J) - photovoltage (V) measurements of the fabricated DSSCs were measured using a laboratory designed automated solar simulator [21]. Philips halogen lamp of 100 W was used as a source of light and its illumination was calibrated to 1000 W/m^2 using NREL calibrated single crystal silicon reference solar cell. Thickness of the TiO_2 film was estimated by gravimetric method using a microbalance with sensitivity of 10 μg [22, 23].

2.4 Synthesis of TiO_2 Nanoparticles

Initially, dry ethanol (14 ml) and distilled water (21 ml) were mixed in a beaker and the mixer was stirred using magnetic stirrer for 15 minutes, at this point without stopping the stirrer action a solution of titanium isopropoxide (7 ml) was added drop wise continuously for five hours until thick solution was obtained. A thick solution so obtained was dried at 70 °C for 2 hours to allow the evaporation of water and ethanol. Then, the product so obtained is subjected for hand milling to get dry powder and consequently sintered at 450 °C for 2 hours to obtain TiO_2 nanoparticles.

2.5 Preparation of Photo-anode

Initially, TiO_2 paste was prepared by taking 0.12 gram of synthesized TiO_2 nanopowder in a crucible containing 150 μl and 250 μl acetyl acetone and ethanol respectively. Later, it was grinded by adding distilled water gradually until distilled water reaches 700 μl. Without stopping the grinding at this point, 60 μl of triton –X100 was added to obtain a fine paste of TiO_2. In order to prepare photo-anode, FTO glass was cleaned with soap water, distilled water and dry ethanol respectively. Then, TiO_2 paste was coated on FTO glass using doctor blading technique. Traces of solvents and additives, as a result of cleaning and coating on FTO glass, were removed by annealing FTO at 550 °C for 45 minutes. This photo-anode was sensitized by RK-1 dye and N-719 dye in ethanol for 12 hour and 24 hour respectively.

2.6 Preparation of Electrolyte

The liquid redox electrolyte is prepared in acetonitrile (ACN) containing a mixture of 0.5 M Lithium Iodide (LiI), 0.05 M Iodine (I_2), 0.5 M 4-tert-Butyl Pyridine (4-TBP) and 0.6 M Di Methyl 3-Propyl ImidAzolium Iodide (DMPII).

2.7 Assembling of DSSCs

The photo-anode sensitized by respective dye as mentioned above was placed on the platinum counter electrode so that the TiO_2 film was sandwiched between the two conducting sides of the FTO glass plates. The glass plates were held tight by binder clips on the two lateral edges. Liquid electrolyte was then injected using small syringe at the interface of two glass plates (electrodes) until electrolyte spreads and adsorbed on the TiO_2 nano porous film by capillary forces.

3. RESULTS AND DISCUSSION

3.1 X-ray Diffraction (XRD) Analysis

XRD is an effective method to analyze crystal structure and crystal size of the samples. Usually TiO_2 crystallizes in three forms namely anatase (tetragonal), brookite (orthorhombic) and rutile (tetragonal). Anatase and brookite forms appear at low temperature however when the same forms of material is heated over 600 °C rutile form appears [24]. Crystal structure can be revealed from TiO_2 XRD pattern which is shown in Fig. 1. From this figure it is observed that peaks appear at (101), (004), (200), (211), (204), (220), (215) and (312) respectively which are the characteristic peaks of TiO_2 nanoparticles. XRD pattern is in good agreement with the JCPDS file of TiO_2 (JCPDS-211272) and observed peaks reveal the anatase and crystalline nature of TiO_2 nanoparticles. The average particle diameter (d) of TiO_2 nanoparticles at most intense peak (101) plane is calculated using Scherrer formula (Eq. (1))

$$d = (0.9\lambda/\beta\cos\theta) \quad (1)$$

where λ is X-ray wavelength of 1.54056 Å, β is full width half maxima and θ is the Bragg's diffraction angle. The estimated average particle diameter (d) of TiO_2 nanoparticles is found to be 7.3 nm.

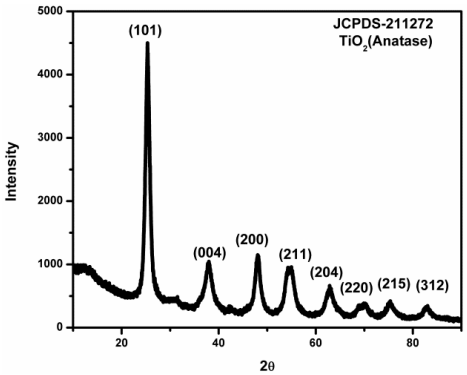

Fig. 1 – XRD pattern of TiO_2 nanoparticles

3.2 Fourier Transform Infrared Spectroscopy (FTIR) Analysis

FTIR is an effective method to analyze the composition of compounds or products. Fig. 2 shows the FTIR spectrum of TiO_2 nanoparticles. From FTIR spectrum of TiO_2 nanoparticles, Ti-O bending mode and deformative vibration of Ti-OH stretching mode may be observed at 483 cm^{-1} and 1623.50 cm^{-1} respectively. Asymmetrical and symmetrical stretching vibrations of hydroxyl group (-OH) may be observed at 3404.82 cm^{-1}. The band at 1623.50 cm^{-1} may be attributed to water adsorbed on TiO_2 surface [1, 24]. These results well agrees with earlier reports.

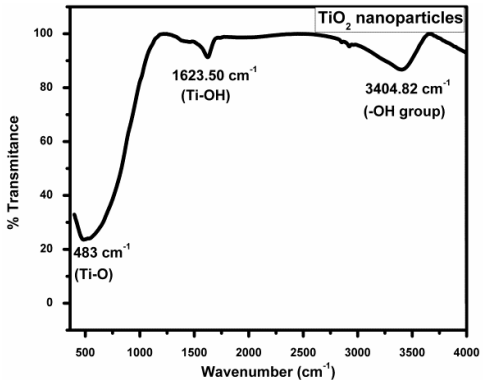

Fig. 2 – FTIR spectrum of TiO_2 nanoparticles

3.3 Scanning Electron Microscope (SEM), Atomic Force Microscopy (AFM) and Energy Dispersive Analysis of X-ray (EDAX) Analysis

The surface morphology and elemental composition of TiO_2 nanoparticles were analyzed from SEM, AFM and EDAX methods. Fig. 3 (a and b) shows SEM images of TiO_2 nanoparticles alone and photo-anode coated with TiO_2 nanoparticles respectively. Fig. 3(c) shows the AFM image of photo-anode coated with TiO_2 nanoparticles. From Fig. 3 (a, b and c) it is observed that the nanoparticles with varying shapes and sizes, uniform distribution and good aggregation with clear porosity. Further, to analyze the composition of TiO_2 nanoparticles, EDAX spectra was recorded and is shown in Fig. 4, the chemical composition in terms of atomic percentage (At%) and weight percentage(Wt%) for different elements are given in Table 1. From Fig. 4 it is seen that, a

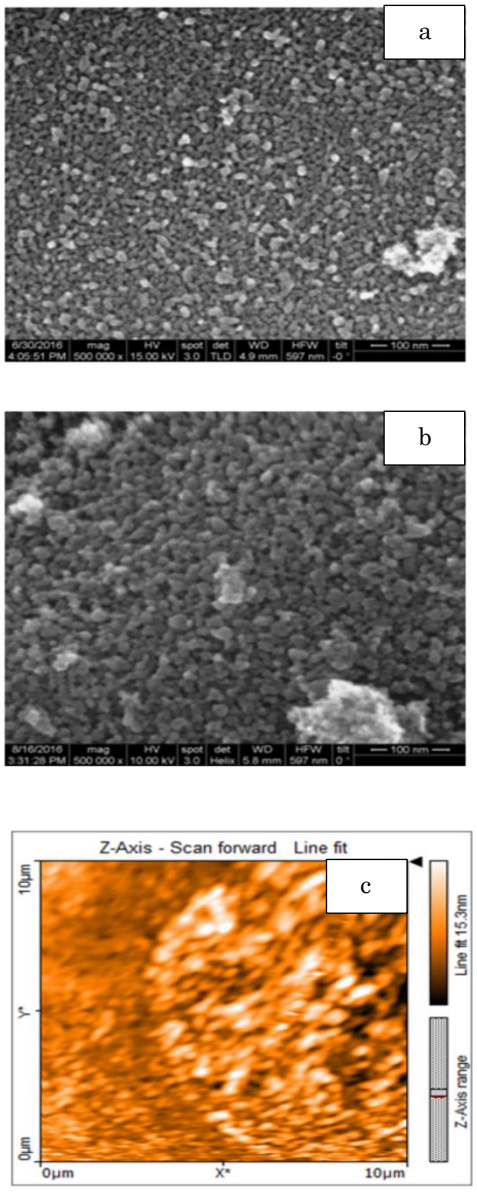

Fig. 3 – SEM Image of (a) TiO_2 nanoparticles alone, (b) photo-anode coated with TiO_2 nanoparticles and (c) AFM image of photo-anode coated with TiO_2 nanoparticles

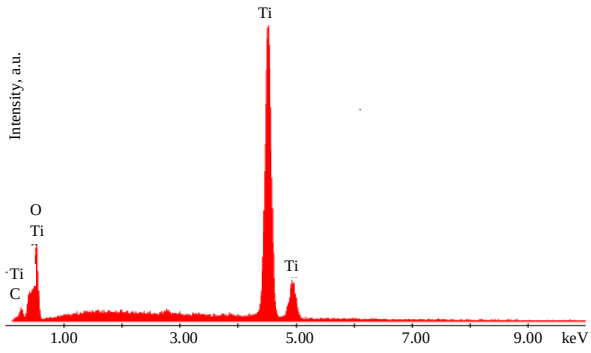

Fig. 4 – Energy dispersive analysis of X-ray (EDAX) spectrum of TiO_2 nanoparticles

Table 1 – Chemical composition of TiO_2 nanoparticles in terms of atomic percentage (At %) and weight percentage (Wt %) from energy dispersive analysis of X-ray (EDAX) measurement

Elements	Atomic percentage (At %)	Weight percentage (Wt %)
Ti	35.34	62.07
O	64.66	37.93
Total	100	100

peak around 0.3 keV of carbon appears which is weak compared to the other peaks such as Ti and O and it is the evidence for purity of synthesized TiO_2 nanoparticles.

3.4 Absorption Spectroscopy Analysis

The absorption measurement of TiO_2 nanoparticles was recorded in distilled water at room temperature using UV-Vis NIR spectrophotometer and normalized absorption spectrum is shown in Fig. 5(a). From Fig. 5(a), it is observed that TiO_2 nano particles absorption peak appears at 261 nm. Fig. 5(b) shows the Plot of $(\alpha hv)^{1/2}$ versus photon energy (hv) of TiO_2 nanoparticles for the wavelengths from 500 to 230 nm and extrapolating the plot, linear relation is obtained [25]. Band gap energy (E_g) of the semiconductor material is determined according to Eq. (2) and is found to be 3.2 eV which is close to the reported value.

$$\alpha hv = A\,(hv - E_g)^{1/2} \qquad (2)$$

where α, hv, E_g and A are absorption coefficient, photon energy (eV), band gap and constant respectively. The normalized absorption spectra of RK-1dye and N-719 dye in ethanol were recorded and shown in Fig. 5(c). From this figure, it is noticed that, RK-1 dye has two intense UV bands corresponding to 208 nm and 338 nm and another band in the visible region corresponding to 467 nm. The bands in the UV region may be as a result of π-π* charge transfer transitions of the conjugated molecules where as a band in the visible region may be due to intramolecular charge transfer (ICT) transition between the electron-donor and electron-acceptor anchoring moieties. In the same figure it is observed that, N-719 dye has two intense UV bands corresponding to 213 nm and 307 nm and two more bands in the visible region corresponding to 382 nm and 523 nm. The bands in the UV region may be as a result of π-π* charge transfer transitions where as the bands in the visible region may be due to metal-to-ligand charge-transfer (MLCT) origin [26].

3.5 Photovoltaic Performance in Dye-sensitized Solar Cells as a Function of TiO_2 Thickness

Photocurrent density (J) versus photovoltage (V) of fabricated DSSCs sensitized with dye as a function of TiO_2 thickness was measured using designed automatic load variable solar simulator [21]. Thickness (t) of the TiO_2 film was estimated by gravimetric method using a microbalance [22, 23] as given by the following Eq. (3).

$$t = \frac{m_1 - m_0}{\rho \times S} \qquad (3)$$

Where, m_0 is the mass of the FTO glass, m_1 is the mass of FTO glass coated with TiO_2 film. S and ρ are the surface area and bulk density of TiO_2 film respectively.

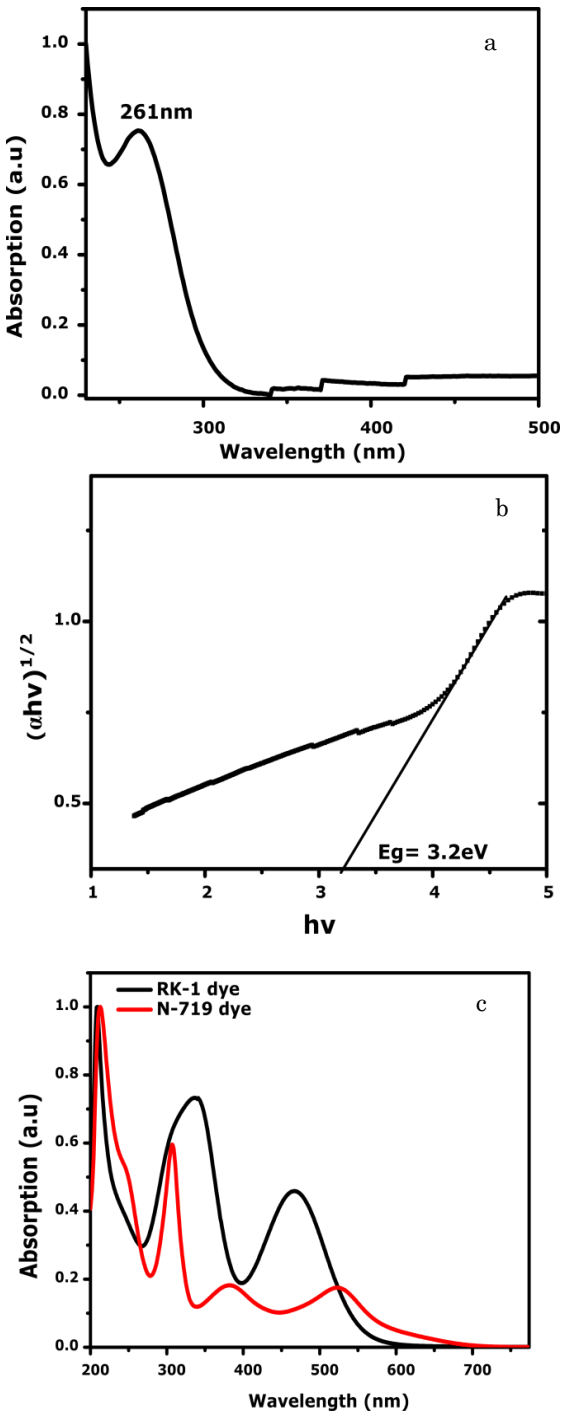

Fig. 5 – (a) Normalized absorption spectrum of TiO_2 nanoparticles, (b) Plot of $(\alpha hv)^{1/2}$ versus photon energy (hv) of TiO_2 nanoparticles and (c) Normalized absorption spectra of RK-1dye and N-719 dye

It is well-known that, photovoltaic performances of DSSCs mainly depend on the film thickness. Thus short circuit current density (J_{sc}) and open circuit voltage (V_{oc}) of respective DSSCs as a function of TiO_2 film thickness are shown in Fig. 6(a) for RK-1 dye and Fig. 6(b) for N-719 dye respectively. Efficiency (η) of respective DSSCs as a function of TiO_2 film thickness are shown in Fig. 7(a) for RK-1 dye and Fig. 7(b) for N-719 dye respectively. In the Fig. 6(a and b) it is observed that, J_{sc} gradually increases to a peak value at

5.4 μm and 8.6 μm thicknesses for RK-1dye and N-719 dye respectively and afterwards gradually decreases. Gradual increase of J_{sc} may be as a result of more absorption of photons as the film thickness increases. However, when the film thickness is beyond the light penetration depth, the number of photons useful for electron photo-generation will reach the limit and therefore, J_{sc} cannot be increased further since increase in the thickness beyond the light penetration depth may yield more recombination centers which results higher electron loss and gradual decrease in J_{sc}. Decrease of J_{sc} may also, be attributed to slower electron injection of dye molecules or self quenching if they undergo aggregation, either before or during dye adsorption on metal oxides [58]. From the same Fig. 6 (a and b) it is observed that, V_{oc} decreases sharply as the thickness of film increases. This may be due to charge recombination and restricted mass transport in the thicker film as a result augmentation of surface area [17, 27, 28].

Fill factor (FF) and photovoltaic conversion efficiency (η) of respective DSSCs are determined according to Eqs. (4) and (5) respectively.

$$FF = \frac{V_{max} \times J_{max}}{J_{sc} \times V_{oc}} \quad (4)$$

$$\eta = \frac{J_{sc} \times V_{oc} \times FF}{I_o} \times 100 \quad (5)$$

where V_{oc} is open circuit voltage, J_{sc} is short circuit current density, V_{max} is maximum power point voltage, J_{max} is maximum power point current density and I_0 is total incident irradiance (I_0 = 1000 W/m^2). V_{oc}, J_{sc}, V_{max} and J_{max} values are obtained from the corresponding J-V plots.

The variation of efficiency (η) as a function of film thickness is shown in Fig. 7(a) for RK-1 dye and Fig. 7(b) for N-719 dye respectively. From Fig. 7(a and b) it is observed that, η gradually increases to peak value at 5.4 μm and 8.6 μm thicknesses for RK-1dye and N-719 dye respectively and afterwards gradually decreases. These figures resembles closely with Fig. 6(a and b) respectively. This may be inferred that J_{sc} is considered as an efficiency-determining parameter since the film thicknesses have shown stronger effect on J_{sc} than on the other photovoltaic parameters [28-30]. Finally, Fig. 8 shows J-V plot for RK-1 dye and N-719 dye with 5.4 μm and 8.6 μm film thicknesses for optimum photovoltaic parameters given in Table 2. Optimum solar energy to electricity conversion efficiencies (η) are 4.08 % and 5.12 % for RK-1 dye and N-719 dye respectively under AM 1.5 irradiation (1000 W/m^2) conditions.

Table 2 – Optimum photovoltaic parameters of best-performing cell with film thickness (Note: Active area of fabricated solar cell was 0.50 cm^2)

Compounds	Thickness (μm)	J_{SC} (mA/cm^2)	V_{OC} (V)	FF	η (%)
RK-1 dye	5.4	12.18	0.675	0.50	4.08
N-719 dye	8.6	13.16	0.740	0.52	5.12

4. CONCLUSIONS

Herein, we have successfully synthesized TiO_2 nanoparticles by sol-gel method. The same was characterized by using, XRD, FTIR, SEM, EDAX, AFM and UV-Vis NIR spectrophotometer. TiO_2 nanoparticles from

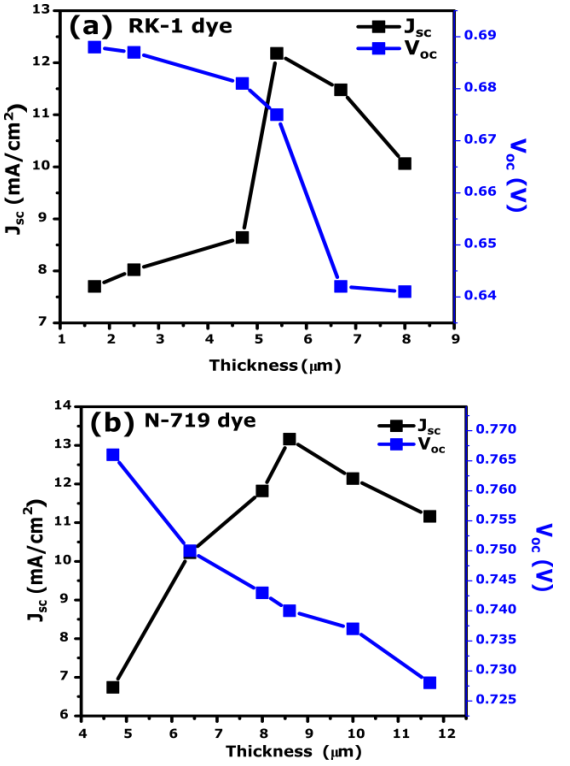

Fig. 6 – Effect of TiO_2 thickness on short circuit current density (black color line indicates J_{sc}) and open circuit voltage (blue color line indicates V_{oc}) (a) for RK-1 dye and (b) for N-719 dye of the fabricated DSSCs

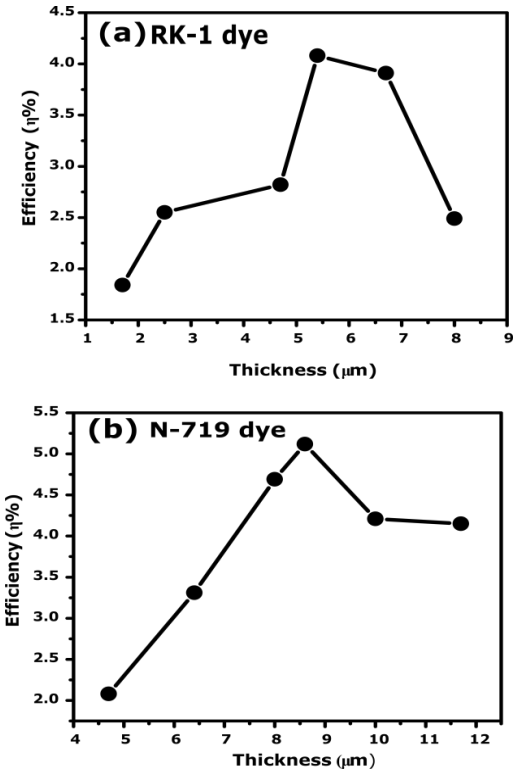

Fig. 7 – The conversion efficiencies (η) of the fabricated DSSCs as a function of TiO_2 thickness (a) for RK-1 dye and (b) for N-719 dye

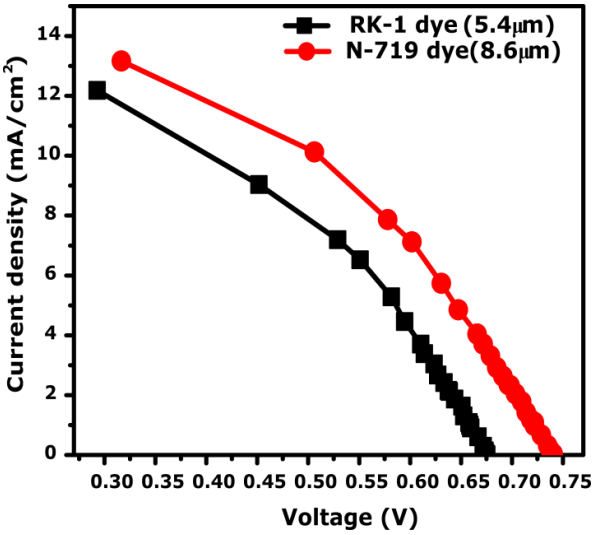

Fig. 8 – Photo-current density (*J*)-photovoltage (*V*) characteristics of the best performed DSSCs (Note: Active area of fabricated solar cell was 0.50 cm²).

XRD and FTIR spectra reveals anatase nature, crystalline structure with average particle size of 7.3 nm and the appearance of Ti-O bending mode at 483 cm^{-1}. SEM and AFM images provide evidence for uniform distribution and good aggregation with clear porosity with varying shapes and sizes. Purity of TiO_2 nanoparticles was confirmed by EDAX result. Band gap of the TiO_2 is determined from absorption spectra and the value agrees well with reported values. DSSCs sensitized by RK-1 and N-719 dyes were fabricated using synthesized TiO_2 nanoparticles. The photovoltaic performance of DSSCs was studied as a function of TiO_2 film thickness. The solar energy conversion efficiencies (η) of DSSCs gradually increases as the thickness of TiO_2 layer increases up to certain thickness, after that it slightly decreases. This may be attributed to more absorption of photons as the film thickness increases as result of more dye adsorption. Solar energy to electricity conversion efficiency (η) for RK-1 and N-719 dyes were of the order 4.08 % and 5.12 % with film thickness of 5.4 μm and 8.6 μm respectively under AM 1.5 irradiation (1000 W/m²) conditions.

ACKNOWLEDGEMENTS

LSC is thankful to Karnatak University, Dharwad (KUD) for UGC-UPE research fellowship. Authors are thankful to Prof N M Badiger, Director, USIC, KUD for facilities like FTIR, UV-Vis spectrophotometer and AFM.

REFERENCES

1. R. Abazari, A.R. Mahjoub, S. Sanati, *RSC Adv.* **4**, 56406 (2014).
2. V.R. Desai, S.M. Hunagund, M.S. Pujar, M. Basanagouda, J.S. Kadadevarmath, A.H. Sidarai, *J. Mol. Liq.* **233**, 166 (2017).
3. B.H. Lee, M.Y. Song, S.Y. Jang, S.M. Jo, S.Y. Kwak, D.Y. Kim, *J. Phys. Chem. C* **113**, 21453 (2009).
4. G.K. Mor, K. Shankar, M. Paulose, O.K. Varghese, C.A. Grimes, *Nano Lett.* **6**, 215 (2006).
5. W.J. Lee, E. Ramasamy, D.Y. Lee, J.S. Song, *ACS Appl. Mater. Interfaces* **1**, 1145 (2009).
6. J. Qu, X.P. Gao, G.R. Li, Q.W. Jiang, T.Y. Yan, *J. Phys. Chem. C* **113**, 3359 (2009).
7. D. Hwang, S.M. Jo, D.Y. Kim, V. Armel, D.R. MacFarlane, S.Y. Jang, *ACS Appl. Mater. Interfaces* **3**, 1521 (2011).
8. M.R. Subramaniam, S. Devanathan, D. Kumaresan, *RSC Adv.* **4**, 36791 (2014).
9. G. Tian, Y. Chen, W. Zhou, K. Pan, C. Tian, X.R. Huang, H. Fu, *CrystalEngComm* **13**, 2994 (2011).
10. K.P. Shejale, D. Laishram, M.S. Roy, M. Kumar, R.K. Sharma, *Mater. Des.* **92**, 535 (2016).
11. A. Latini, C. Cavallo, F.K. Aldibaja, D. Gozzi, D. Carta, A. Corrias, L. Lazzarini, G. Salviati, *J. Phys. Chem. C* **117**, 25276 (2013).
12. B. Roose, S. Pathak, U. Steiner, *Chem. Soc. Rev.* **44**, 8326 (2015).
13. Y. Cui, L. Zhang, K. Lv, G. Zhou, Z.S. Wang, *J. Mater. Chem. A* **3**, 4477 (2015).
14. J.T. Park, D.K. Roh, R. Patel, E. Kim, D.Y. Ryu, J.H. Kim, *J. Mater. Chem.* **20**, 8521 (2010).
15. E.V. Savinkina, G.M. Kuzmicheva, N.Y. Tabachkova, L.N. Obolenskaya, P.A. Demina, A.G. Yakovenko, *Inorg. Mater.* **47**, 556 (2011).
16. D. Hwang, D.Y. Kim, S.Y. Jang, D. Kim, *J. Mater. Chem. A* **1**, 1228 (2013).
17. P. Balraju, P. Suresh, M. Kumar, M.S. Roy, G.D. Sharma, *J. Photochem. Photobiol. A* **206**, 53 (2009).
18. E.V. Savinkina, G.M. Kuzmicheva, N.Yu. Tabachkova, L.N. Obolenskaya, P.A. Demina, A.G. Yakovenko, *Inorg. Mater.* **47**, 489 (2011).
19. M.K. Nazeeruddin, A. Kay, I. Rodicio, R. Humphry-Baker, E. Muller, P. Liska, N. Vlachopoulos, M. Gratzel, *J. Am. Chem. Soc.* **115**, 6382 (1993).
20. C.J. Barbe, F. Arendse, P. Comte, M. Jirousek, F. Lenzmann, V. Shklover, M. Gratzel, *J. Am. Ceram. Soc.* **80**, 3157 (1997).
21. M.S. Yatnatti, R.K. Linganagoudar, J.S. Kadadevarmath, *Global Research Analysis* **2**, 1 (2013).
22. J.S. Bhat, K.I. Maddani, A.M. Karguppikar, *Bull. Mater. Sci.* **29**, 331 (2006).
23. J.S. Bhat, A.S. Patil, N. Swami, B.G. Mulimani, B.R. Gayathri, N.G. Deshpande, G.H. Kim, M.S. Seo, Y.P. Lee, *J. Appl. Phys.* **108**, 043513 (2010).
24. Z. Antic, R.M. Krsmanovic, M.G. Nikolic, M.M. Cincovic, M. Mitric, S. Polizzi, M.D. Dramicanin, *Mater. Chem. Phys.* **135**, 1064 (2012).
25. M. Caglar, S. Ilican, Y. Caglar, *Thin Solid Films* **517**, 5023 (2009).
26. Md.K. Nazeeruddin, R. Splivallo, P. Liska, P. Comte, M. Gratzel, *Chem. Commun.* 1456 (2003).
27. V. Thavasi, V. Renugopalakrishnan, R. Jose, S. Ramakrishna, *Mater. Sci. Eng.* **63**, 81 (2009).
28. R. Gomez, P. Salvador, *Sol. Energ. Mater. Sol. C.* **88**, 377 (2005).
29. W.C. Chang, C.H. Lee, W.C. Yu, C.M. Lin, *Nanoscale Res. Lett.* **7**, 688 (2012).
30. H. Horiuchi, R. Katoh, K. Hara, M. Yanagida, S. Murata, H. Arakawa, M. Tachiya, *J. Phys. Chem. B* **107**, 2570 (2003).